Linkage Isomerizations of (Sulfoxide)ammineruthenium Complexes Induced by Electrochemical Processes

Atsuko Tomita and Mitsuru Sano*

Graduate School of Human Informatics, Nagoya University, and PRESTO-21 Project, JRDC, Nagoya 464-01, Japan

Received March 30, 1994[⊗]

The redox behavior in acetone solution of $[Ru(NH_3)_5(sulfoxide)]^{2+/3+}$ and *cis*-$[Ru(NH_3)_4(dmso)_2]^{2+/3+}$, where linkage isomerizations, $Ru^{III}S\rightarrow O$ and $Ru^{II}O\rightarrow S$, are brought about by electrochemical oxidation or reduction has been characterized, and the first-order rate constants for them have been obtained. In the isomerization of $Ru^{III}S\rightarrow O$, a bulky substituent group on the S atom accelerates the reaction over 1000 s^{-1} for $[Ru(NH_3)_5$(*sec*-butyl sulfoxide)$]^{3+}$ from 0.4 s^{-1} for $[Ru(NH_3)_5(dmso)]^{3+}$. In *cis*-$[Ru(NH_3)_4(dmso)_2]^{3+}$, the rate of the $Ru^{III}SS\rightarrow SO$ is much faster than 1000 s^{-1} at room temperature. Substitution on the S atom barely changes the isomerization rates (~10 s^{-1}) for the $Ru^{II}O\rightarrow S$ of the $[Ru(NH_3)_5(sulfoxide)]^{2+}$ complexes. However, the replacement of a *cis*-ammine by pyridine reduces the rate to 0.7 s^{-1}. We obtained the related thermodynamic parameters in the dmso, the *n*-butyl sulfoxide, and the (1,5-dithiacyclooctane 1-oxide)ruthenium complexes and also determined the reaction scheme. The thermodynamics is also presented in for *cis*-$[Ru(NH_3)_4(dmso)_2]^{2+/3+}$.

Introduction

Our special interest in isomerizations brought about by redox processes derives from the fact that they are selectively triggerable by the application of suitable potentials. Each system remains in a state Z_1 until addressed by trigger signal whereupon it assumes the state Z_2^+. Systems of this kind are the key building block of all digital electronic devices.[1] Scheme 1 outlines the succession of events in completing a redox cycle for such a system. It is characterized by two redox potentials E_1 and E_2, two chemical reactions for each case with the rate constants k_1 and k_2.

The redox couples Z_1/Z_1^+ and Z_2/Z_2^+ are in principle reversible; however, if the isomerization following electron transfer is sufficiently rapid, the electron transfer becomes irreversible. Since Z_1 and Z_2 differ in chemical constitution, E_1 and E_2 can differ. In electroanalytical terminology this is designated an ECEC system,[2] which is switched by the comparatively trivial recharging. As an unexplored application, we speculate that the triggerable linkage isomerizations can direct molecular motions and can be the engine of a molecular machine.

We previously reported a (sulfoxide)ruthenium dinuclear complex whose redox behavior shows "molecular hysteresis",[3a,b] a phenomenon implying memory in a molecule and, in principle, applicable to a high density memory storage. It is based on rapid isomerization in the oxidation state and slow intramolecular electron transfer between two ruthenium complexes.

Linkage isomerization of sulfoxidepentaammineruthenium complexes was first reported by Yeh et al.[4] In the stable forms, sulfoxide is bound via S to Ru(II)[5] and via O to Ru(III).[6] When the S-bond isomer is oxidized at 1.0 V, linkage isomerization occurs to the more stable O-bond form. When the resulting species is reduced at 0.0 V, it rearranges to the more stable original state. The rates at 25 °C and aqueous solution are 0.07 and 0.24 s^{-1} for the $S\rightarrow O$ isomerization and 30 s^{-1} and 90 s^{-1} for the $O\rightarrow S$ in dimethyl sulfoxide (dmso) and methionine sulfoxide complexes in aqueous solutions, respectively.[4]

Scheme 1

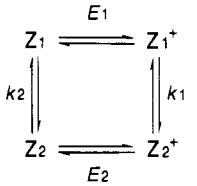

In order to apply linkage isomerization to the broader fields referred to above, variable rates of linkage isomerization are needed. In line with this, we have undertaken to learn the effect on these rates of changing the substituents on the sulfur and of changing the coligands and to determine the energy differences between the isomeric forms.

To this end, we have prepared a series of (sulfoxide)-ammineruthenium and measured the rates and free energies for the isomerizations of the complexes.

Experimental Section

Materials. $[Ru(NH_3)_5(acetone)](PF_6)_2$ and *cis*-$[Ru(NH_3)_4(acetone)_2](PF_6)_2$ were synthesized from $[Ru(NH_3)_5Cl]Cl_2$ and *cis*-$[Ru(NH_3)_4Cl_2]Cl$ as described in the literature,[7a,b] respectively. $[Ru(NH_3)_5(sos)](PF_6)_2$ (sos; 1,5-dithiacyclooctane 1-oxide),[3b] $[Ru(NH_3)_5$(*p*-fluorobenzonitrile)$](PF_6)_2$,[8] and $[Ru(NH_3)_5$(2,6-difluorobenzonitrile)$](PF_6)_2$[8] were synthesized as described in the literature. Diphenyl sulfoxide (dpso), dibenzyl sulfoxide (benzylso), bis(4-chlorophenyl) sulfoxide (Cl-pso), and di-*n*-butyl sulfoxide (*n*-buso) were recrystallized from proper solvents.

Bis(chloromethyl) sulfoxide (Cl-mso),[9a] di-*tert*-butyl sulfoxide (*t*-buso),[9b] di-*sec*-butyl sulfoxide (*s*-buso),[9b] and sos[9c] were synthesized

[⊗] Abstract published in *Advance ACS Abstracts,* September 15, 1994.

(1) Kölle, U. *Angew. Chem., Int. Ed. Engl.* **1991**, *30*, 956.
(2) (a) Bard, A. J.; Faulkner, L. R. *Electrochemical Methods: Fundamentals and Applications*; Wiley: New York, 1980. (b) Heinze, J. *Angew. Chem., Int. Ed. Engl.* **1984**, *23*, 831. (c) Geiger, W. E. *Prog. Inorg. Chem.* **1985**, *33*, 275.
(3) (a) Sano, M.; Taube, H. *J. Am. Chem. Soc.* **1991**, *113*, 2327. (b) Sano, M.; Taube, H. *Inorg. Chem.* **1994**, *33*, 705.
(4) Yeh, A.; Scott, N.; Taube, H. *Inorg. Chem.* **1982**, *21*, 2542.
(5) March, F. C.; Ferguson, G. *Can. J. Chem.* **1971**, *49*, 3590.
(6) Tomita, A.; Sano, M. To be submitted for publication. A single crystal X-ray analysis has been performed for $[Ru(NH_3)_5(dmso)](CF_3SO_3)_3$. The oxygen of the dmso has been confirmed to coordinate to the Ru^{III}.
(7) (a) Callahan, R. W.; Brown, G. M.; Meyer, T. J. *Inorg. Chem.* **1975**, *14*, 1443. (b) Sugaya, T.; Sano, M. *Inorg. Chem.* **1993**, *32*, 5878.
(8) Takemoto, M.; Sugaya, T.; Tomita, A.; Sano, M. To be submitted for publication.
(9) (a) Mann, F. G.; Pope, W. J. *J. Chem. Soc., Trans.* **1923**, *123*, 1172. (b) Drabowicz, J.; Lyzwa, P.; Popielarczyk, M.; Mikolajczyk, M. *Synthesis* **1990**, 937. (c) Roush, O. B.; Musker, W. K. *J. Org. Chem.* **1978**, *43*, 4295.

0020-1669/94/1333-5825$04.50/0

as described in the literature. Dimethyl sulfoxide (dmso) and tetramethylene sulfoxide (tmso) were purchased from Wako Chemical and Tokyo Kasei, respectively, and were used without further purification. Acetone was purified by vacuum distillation over B_2O_3.[10] Anhydrous Et_2O and CH_2Cl_2 were purchased from Aldrich (Sure/Seal bottle) and were used without further purification. Tetra-1-butylammonium hexafluorophosphate (n-Bu_4NPF_6) (Tokyo Kasei) was twice recrystallized from ethanol and dried at 105 °C under vacuum. All solvents were thoroughly deoxygenated by purging with argon in a Vacuum/Atmospheres Co. inert atmosphere dry glovebox.

Instrumentation. Proton and carbon-13 NMR spectra were recorded on a JEOL EX-270 spectrometer and are reported as ppm shifts from acetone-d_6 (2.04 ppm for ^1H and 29.8 ppm for ^{13}C). The electronic absorption spectra were recorded on a Hitachi 330 spectrophotometer.

Bulk electrolysis and coulometry experiments were performed on a PAR Model 173 potentiostat with a PAR Model 276A interface, which was driven by a PAR Model 175 universal programmer. Cyclic voltammetry with a thin layer cell and differential pulse voltammetry were carried out by BAS-100B on acetone solutions of complexes (10 mM). Electrochemical experiments were performed by a three-electrode system with a platinum working electrode, a platinum-wire counter electrode, and a gold-wire reference electrode with ferrocene/ferrocenium hexafluorophosphate (Fc/Fc^+) dissolved in acetone. In thin layer cyclic voltammograms, a platinum mesh (150 mesh) was used. In all acetone solutions, concentrations of n-Bu_4NPF_6 are 0.2 M. Cyclic voltammograms at fast scan rates (1.0−1000 V s^{-1}) and double potential step experiments were recorded on a Riken Denshi transient recorder TCFL-8000E. All potentials are reported vs the normal hydrogen electrode. The reference electrode was calibrated with the ferrocene−ferrocenium couple (E = 0.55 V (NHE)) as measured in situ. Variable temperature electrochemical experiments in the drybox employed a thermostat system with EYELA MPF-40, which controlled the temperature to ±0.1 K.

All reactions and measurements were carried out under argon atmosphere in a Vacuum/Atmospheres Co. inert atmosphere dry glovebox.

General Preparation of [Ru(NH$_3$)$_5$(sulfoxide)](PF$_6$)$_2$. In a typical preparation, 100 mg of $[Ru(NH_3)_5(acetone)](PF_6)_2$ was dissolved in 3 mL of acetone. The desired sulfoxide was added at four times the concentration of the complex, and the solution was stirred for 20 min. The solution was treated with about 2 mL of CH_2Cl_2, and the resulting precipitate was filtered off. The filtrate was treated with CH_2Cl_2, and the solid was filtered off. The solid was redissolved with acetone, and then the solution was again treated with CH_2Cl_2. The precipitate was filtered off and washed with CH_2Cl_2 and ether.

The compounds were characterized by ^1H NMR, cyclic voltammetry, and elemental analysis.

[Ru(NH$_3$)$_5$(dmso)](PF$_6$)$_2$. ^1H NMR (acetone-d_6): δ 3.70 (br, 3H, *trans*-NH3), 3.33 (s, 6H), 2.55 (br, 12H, *cis*-NH_3). Cyclic voltammetry (acetone, 0.2 M n-Bu_4NPF_6, 100 mV/s): E_{pa} = 1.01 V, E_{pc} = 0.06 V. UV/vis (H_2O): 312, 234 (sh), 211 nm.

Anal. Calcd for $C_2H_{21}N_5SORuP_2F_{12}$: C, 4.32; H, 3.81; N, 12.61. Found: C, 4.70; H, 3.77; N, 12.61.

[Ru(NH$_3$)$_5$(tmso)](PF$_6$)$_2$. ^1H NMR (acetone-d_6): δ 3.74 (br, 3H, *trans*-NH_3), 3.5−3.4 (m, 2H), 3.3−3.2 (m, 2H), 2.58 (br, 12H, *cis*-NH_3), 2.4 (m, 2H), 2.2 (m, 2H). Cyclic voltammetry (acetone, 0.2 M n-Bu_4NPF_6, 100 mV/s): E_{pa} = 1.00 V, E_{pc} = 0.03 V. UV/vis (H_2O): 315, 215 nm.

Anal. Calcd for $C_4H_{23}N_5SORuP_2F_{12}$: C, 8.26; H, 3.99; N, 12.05. Found: C, 8.41; H, 3.89; N, 12.26.

[Ru(NH$_3$)$_5$(dpso)](PF$_6$)$_2$. ^1H NMR (acetone-d_6): δ 7.9−7.8 (m, 4H), 7.6−7.5 (m, 6H), 3.95 (br, 3H, *trans*-NH_3), 2.68 (br, 12H, *cis*-NH_3). Cyclic voltammetry (acetone, 0.2 M n-Bu_4NPF_6, 100 mV/s): E_{pa} = 1.11 V, E_{pc} = 0.16 V. UV/vis (H_2O): 332, 272 (sh), 264 (sh), 256 nm.

Anal. Calcd for $C_{12}H_{25}N_5SORuP_2F_{12}$: C, 21.21; H, 3.71; N, 10.31. Found: C, 21.90; H, 3.65; N, 10.46.

[Ru(NH$_3$)$_5$(benzylso)](PF$_6$)$_2$. In this preparation, the volume of acetone was reduced to 1 mL, because the complex has high solubilty in acetone. ^1H NMR (acetone-d_6): δ 7.47 (m, 4H), 7.40 (m, 4H), 4.72 (q, 4H, CH_2) 3.61 (br, 3H, *trans*-NH_3), 2.40 (br, 12H, *cis*-NH_3). Cyclic voltammetry (acetone, 0.2 M n-Bu_4NPF_6, 100 mV/s): E_{pa} = 1.09 V, E_{pc} = 0.16 V. UV/vis (H_2O): 322, 254 (sh), 219 nm.

Anal. Calcd for $C_{19}H_{29}N_5SORuP_2F_{12}$: C, 23.76; H, 4.13; N, 9.90. Found: C, 23.81; H, 4.19; N, 9.74.

[Ru(NH$_3$)$_5$(Cl-pso)](PF$_6$)$_2$. Volume of acetone: 1 mL. ^1H NMR (acetone-d_6): δ 7.9-7.8 (m, 4H), 7.6−7.5 (m, 4H), 4.00 (br, 3H, *trans*-NH_3), 2.72 (br, 12H, *cis*-NH_3). Cyclic voltammetry (acetone, 0.2 M n-Bu_4NPF_6, 100 mV/s): E_{pa} = 1.17 V, E_{pc} = 0.19 V. UV/vis (H_2O): 331, 269 (sh), 235 nm.

Anal. Calcd for $C_{12}H_{23}N_5Cl_2SORuP_2F_{12}$: C, 19.26; H, 3.10; N, 9.36. Found: C, 19.12; H, 3.09; N, 9.24.

[Ru(NH$_3$)$_5$(Cl-mso)](PF$_6$)$_2$. ^1H NMR (acetone-d_6): δ 5.38 (q, 4H, CH_2), 4.03 (br, 3H, *trans*-NH_3), 2.81 (br, 12H, *cis*-NH_3). Cyclic voltammetry (acetone, 0.2 M n-Bu_4NPF_6, 100 mV/s): E_{pa} = 1.29 V, E_{pc} = 0.23 V. UV/vis (H_2O): 312, 252 (sh), 225 nm.. Anal. Calcd for $C_2H_{19}N_5Cl_2SORuP_2F_{12}$: C, 3.85; H, 3.07; N, 11.22. Found: C, 4.03; H, 2.87; N, 10.82.

[Ru(NH$_3$)$_5$(*n*-buso)](PF$_6$)$_2$. Volume of acetone: 1 mL. The solution of the complex was treated with CH_2Cl_2 because treatment with ether gave an oil. ^1H NMR (acetone-d_6): δ 3.66 (br, 3H, *trans*-NH_3), 3.44 (m, 4H, CH_2), 2.58 (br, 12H, *cis*-NH_3), 1.84 (m, 4H, CH_2), 1.47 (m, 4H, CH_2), 0.94 (t, 3H, CH_3). Cyclic voltammetry (acetone, 0.2 M n-Bu_4NPF_6, 100 mV/s): E_{pa} = 1.02 V, E_{pc} = 0.07 V. UV/vis (H_2O): 320, 237 (sh), 212 nm.

Anal. Calcd for $C_8H_{33}N_5SORuP_2F_{12}$: C, 15.02; H, 5.20; N, 10.95. Found: C, 15.09; H, 4.95; N, 10.83.

[Ru(NH$_3$)$_5$(*s*-buso)](PF$_6$)$_2$. The reaction time was 5 min. The first precipitation was with ether. ^1H NMR (acetone-d_6): δ 3.65 (br, 3H, *trans*-NH_3), 3.55 (m, 2H, CH), 2.65 (br, 12H, *cis*-NH_3), 1.7−1.6 (m, 4H, CH_2), 1.39 (q, 6H, CH_3), 1.05 (q, 6H, CH_3). Cyclic voltammetry (acetone, 0.2 M n-Bu_4NPF_6, 100 mV/s): E_{pa} = 0.98 V, E_{pc} = 0.10 V. UV/vis (H_2O): 331, 242 (sh), 219 nm.

Anal. Calcd for $C_8H_{33}N_5SORuP_2F_{12}$: C, 15.02; H, 5.20; N, 10.95. Found: C, 15.00; H, 4.75; N, 10.88.

Preparation of *cis*-[Ru(NH$_3$)$_4$(dmso)$_2$](PF$_6$)$_2$. One hundred milligrams of *cis*-$[Ru(NH_3)_4(acetone)_2](PF_6)_2$ was dissolved in 1 mL of acetone. An excess of the dmso (115 mg) was added, and the solution was stirred for 30 min and then treated with CH_2Cl_2. The resulting precipitate was filtered off and was washed with CH_2Cl_2. The solid was redissolved with acetone, and then the solution was treated with CH_2Cl_2. The resulting precipitate was filtered off and washed with CH_2Cl_2. ^1H NMR (acetone-d_6): δ 3.47 (br, 6H, NH_3), 3.41 (m, 12H, CH_3), 2.95 (br, 6H, NH_3). Cyclic voltammetry (acetone, 0.2 M n-Bu_4NPF_6, 100 mV/s): E_{pa} = 1.70 V, E_{pc} = 0.98, 0.02 V: UV/vis (H_2O): 320 (sh), 292, 226 (sh) nm.

Anal. Calcd for $C_4H_{24}N_4S_2O_2RuP_2F_{12}$: C, 7.79; H, 3.92; N, 9.08. Found: C, 8.00; H, 3.77; N, 9.15.

Preparation of *cis*-[Ru(NH$_3$)$_4$(pyridine)(dmso)](PF$_6$)$_2$·dmso. One hundred-seventy-eight milligrams of *cis*-$[Ru(NH_3)_4(acetone)_2](PF_6)_2$ was dissolved in 0.5 mL of acetone. Then dmso (26 mg) in 1.5 mL of acetone was added, and the solution was stirred for 5 min. The solution was treated with CH_2Cl_2. The solid was dissolved in 2 mL of acetone. Pyridine (750 mg) was added, and the solution was stirred for 60 min, and then treated with CH_2Cl_2. The resulting precipitate was filtered off and washed with CH_2Cl_2. The solid was redissolved with acetone, and the solution was treated with CH_2Cl_2. The resulting precipitate was filtered off and washed with CH_2Cl_2. ^1H NMR (acetone-d_6): δ 8.79 (d, 2H), 7.96 (t, 1H), 7.51 (t, 2H), 3.74 (br, 3H, *trans*-NH_3), 3.22 (s, 6H, CH_3), 2.95 (br, 3H, *trans*-NH_3), 2.82 (br, 6H, *cis*-NH_3). Cyclic voltammetry (acetone, 0.2 M n-Bu_4NPF_6, 100 mV/s): E_{pa} = 1.18 V, E_{pc} = 0.28 V. UV/vis (H_2O): 321, 238 nm.

Anal. Calcd for $C_{10}H_{29}N_5SO_2RuP_2F_{12}$: C, 17.78; H, 4.32; N, 10.36. Found: C, 17.18; H, 3.93; N, 10.33.

Kinetic and Thermodynamic Experiments. The double potential step chronoamperometry (DPSCA) method of Schwarz and Shain[11] for EC systems was used to calculate the rate constants for the isomerization reactions. We chose DPSCA as the best method to determine the isomerization rates.[2c] A typical DPSCA is deserved in the following: 1 mL of a 10 mM solution of a complex in 0.2 M (TBA)PF_6/acetone

(10) Burfield, D. R.; Smithers, R. H. *J. Org. Chem.* **1978**, *43*, 3966.

(11) Schwarz, W. M.; Shain, I. *J. Phys. Chem.* **1965**, *69*, 30.

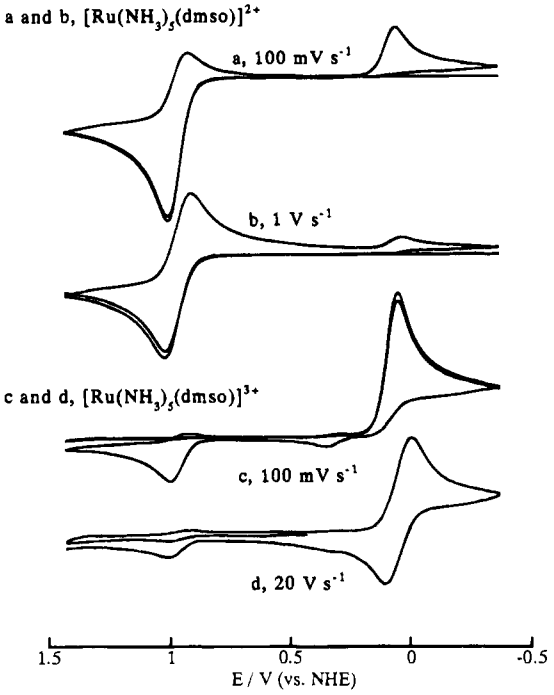

Figure 1. Cyclic voltammograms on acetone solutions containing $[Ru(NH_3)_5(dmso)]^{2+/3+}$ (10 mM dm^{-3}) and *n*-Bu_4NPF_6 (0.1 M dm^{-3}) at 20 °C.

was admitted to the working electrode compartment of the electrochemical cell. A cyclic voltammogram was taken on the solution to determine whether the system was performing well and to determine the oxidizing and reducing potentials for the DPS experiments. The stepping potentials were chosen as 400 mV positive and negative of *E*pa and *E*pc, respectively. DPSCA experiments were then recorded for forward proper stepping times, τ. The cell was then emptied and refilled with an identical solution and the experiment repeated. To obtain the background currents, the cell was emptied, rinsed, and refilled with only the electrolyte solution and the experiment repeated. Current ratios, $ir(t + \tau)/if(t)$, for t/τ values of 0.2 were obtained by measuring the currents and subtracting the corresponding background currents. To keep the current ratios 0.3−0.4, we set the stepping time, τ, to range from 0.4 ms to 20 s. The proper working platinum electrode (r = 0.2, 0.5, 1.0 mm) was selected to roughly keep current constant during time τ. Kinetic parameters were obtained from the theoretical working curve of Schwarz and Shain[11] and were averaged from at least three measurements. Standard deviations in all cases were less than 3%.

Digital Simulation for Cyclic Voltammetry. Digital simulations of proposed electrochemical mechanisms were done with a general purpose program[12] designed to simulate voltammograms for any mechanism formulated as a combination of heterogeneous charge transfer and homogeneous reactions. We assumed Nernstian behavior in this simulation. The input for the simulations consisted of oxidation−reduction voltages and forward and reverse rate constants for each homogeneous reaction.

Results and Discussion

Overviews of Cyclic Voltammetry for $[Ru(NH_3)_5(dmso)]^{2+/3+}$. Yeh et al.[4] reported the S to O and the O to S linkage isomerizations in $[Ru(NH_3)_5(sulfoxide)]^{2+/3+}$, but they did not publish any figures of cyclic voltammograms. We now introduce the cyclic voltammograms for $[Ru(NH_3)_5(sulfoxide)]^{2+/3+}$.

The cyclic voltammetry of $[Ru(NH_3)_5(dmso)]^{2+}$ exhibits an oxidation wave at 1.01 V (vs NHE) and a reduction wave at 0.06 V (Figure 1A) at slow scan rates (<100 mV s^{-1}) and at

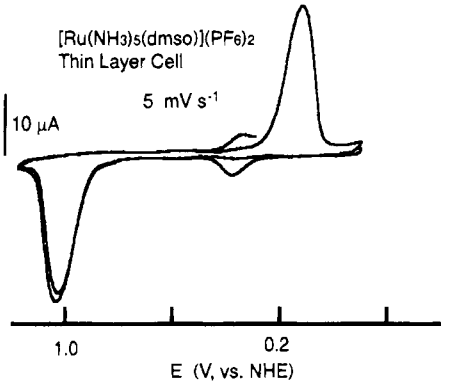

Figure 2. Thin layer cyclic voltammogram recorded at a platinum mesh electrode on an acetone solution containing $[Ru(NH_3)_5(dmso)](PF_6)_2$ (10 mM dm^{-3}) and *n*-Bu_4NPF_6 (0.1 M dm^{-3}) at 5 mV s^{-1}.

20 °C. A similar response is obtained from the cyclic voltammetry of $[Ru(NH_3)_5(dmso)]^{3+}$, at slow scan rates (<100 mV s^{-1}) (Figure 1C). However, at higher scan rates, both complexes display reversible cyclic voltammograms; for $[Ru(NH_3)_5(dmso)]^{2+}$ at 1 V s^{-1}, a couple is observed at 0.97 V, while for $[Ru(NH_3)_5(dmso)]^{2+}$ at 20 V s^{-1}, a couple is observed at 0.07 V (Figures 1B, D). The scan-rate-dependent reversibility noted above is characteristic of an ECEC mechanism.[2a,b,c] Oxidation-state-dependent linkage isomerizations in which there is an isomerization of the sulfoxide ligand to S-coordination upon oxidation and a corresponding isomerization to O-coordination upon reduction are being observed.[5,6]

Obtaining a thin layer cyclic voltammogram is one of the best ways to verify the reversibility of the conversions between the two chemical forms in the system because bulk electrolysis can be carried out in the thin layer cell. The behavior of the system is shown in Figure 2. On scanning to an oxidation potential high enough to oxidize the ruthenium(II)-sulfoxide, we observe an oxidation wave at 0.97 V without any corresponding reduction wave. When one scans to a reduction potential, there is a single irreversible reduction wave at 0.06 V with the same amplitude as the oxidation wave, which shows that Ru(III)−S has been completely converted to Ru(III)−O forms. On the forward scan again, we find a small reversible oxidation wave at 0.3 V corresponding to the bis(acetone) complex and the irreversible oxidation wave at 0.97 V with a rather small amplitude as in the last scan. In multiscan thin layer cyclic voltammograms, amplitude of the reversible wave at 0.3 V increases and amplitude of the waves at 0.97 and 0.06 V decreases. A small amount of impurity is generated after the reduction of Ru(III)−O.

We turn now to a consideration of the electronic structure of sulfoxides, taking dmso as a simplest example. DV−Xα MO[13] calculation gives as the HOMO (21st orbital), which is roughly characterized as a lone pair on the S atom. The LUMO is also located on the S atom. A lone-pair orbital localized on the O atom is the 19th-MO, and it is lower an energy than the HOMO by 5.7 eV. The moiety $Ru(NH_3)_5^{2+}$ is well-known to be electron-rich,[14] which implies that the πd orbitals of ruthenium(II) are high in energy. As a result, the HOMO and the LUMO of dmso can easily interact with the metal d-orbital through σ-bonding and π-bonding, respectively. When the Ru(II) is oxidized to the Ru(III), the metal d-orbital lowers and easily mixes with the lower oxygen lone-pair orbital. This is why the Ru(II) favors the S atom and the Ru(III) the O atom.

(12) (a) Feldberg, S. W. *Electroanal. Chem.* **1969**, *3*, 199. (b) Magno, F.; Bontempelli, G.; Andreuzzi-Sedea, M. *Anal. Chim. Acta* **1982**, *140*, 65.

(13) Adaci, H.; Shiokawa, S.; Tsukada, M.; Satoko, C. *J. Phys. Soc. Jpn.* **1979**, *47*, 1528.

(14) Taube, H. *Pure Appl. Chem.* **1979**, *51*, 901.

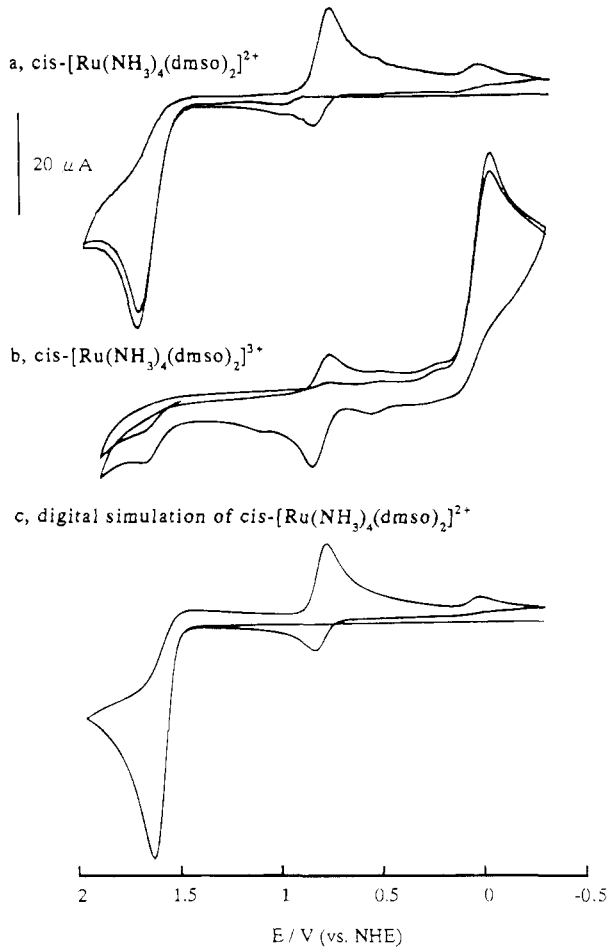

Figure 3. Cyclic voltammograms on acetone solutions containing *cis*-$[Ru(NH_3)_4(dmso)_2]^{2+/3+}$ (10 mM dm^{-3}) and *n*-Bu_4NPF_6 (0.1 M dm^{-3}) at 100 mV s^{-1} at 20 °C and a digital simulation for *cis*-$[Ru(NH_3)_4(dmso)_2]^{2+}$.

Electrochemistry of *cis*-$[Ru(NH_3)_4(sulfoxide)_2]^{2+/3+}$. The cyclic voltammetry of *cis*-$[Ru(NH_3)_4(dmso)_2]^{2+}$ exhibits an oxidation wave at 1.7 V, one reduction wave at 0.78 V, and one more small reduction wave at 0.02 V (Figure 3A) at 100 mV s^{-1} and at 20 °C. A similar response is obtained from the cyclic voltammetry of *cis*-$[Ru(NH_3)_4(dmso)_2]^{3+}$, at 100 mV s^{-1} (Figure 3B).

The potentials at 0.0 and 0.8 V are close to those of the $[Ru(NH_3)_5(O)]^{3+/2+}$ and $[Ru(NH_3)_5(S)]^{2+/3+}$ complexes, respectively for dmso as ligand. Since the reduction potentials of $[Ru(NH_3)_6]^{3+}$ and $[Ru(NH_3)_5(O)]^{3+}$ are almost identical at 0.05 V, the reduction potential of ruthenium ammine complexes remains substantially unchanged by substitution of a O(sulfoxide) for NH_3, which suggests that the reduction potential of the O-coordination of bis(sulfoxide)tetraammineruthenium, *cis*-$[Ru(NH_3)_4(O)_2]^{3+}$, should be close to that of $[Ru(NH_3)_5(O)]^{3+}$. The reduction wave at 0.0 V can be assigned to the reduction of *cis*-$[Ru(NH_3)_4(O)_2]^{3+}$. Continuing the agreement, the wave at 0.8 V can be assigned to the redox of the O-coordination and S-coordination of bis(sulfoxide)tetraammineruthenium, *cis*-$[Ru(NH_3)_4(S)(O)]^{3+/2+}$, and the oxidation wave at 1.7 V to the oxidation of the S-coordination of bis(sulfoxide)tetraammineruthenium, *cis*-$[Ru(NH_3)_4(S)_2]^{2+}$.

Rate Constants for Isomerizations of $[Ru(NH_3)_5(dmso)]^{3+/2+}$ as a Function of Concentration. The rate constants, k_1, for the S→O linkage isomerization of $[Ru(NH_3)_5(dmso)]^{3+}$ were measured at three different concentrations of the complexes, 2.1, 10, and 98 mM and yielded the values 0.35, 0.37, and 0.37 s^{-1}, respectively. We also measured the rate constants, k_2, for the O→S linkage isomerization of $[Ru(NH_3)_5(dmso)]^{2+}$ where the values 13 s^{-1} for 4.3 mM, 14 s^{-1} for 10 mM, and 13 s^{-1} for 150 mM were obtained. For any square reaction scheme, there exists the added complication of intermolecular electron transfer, where the minor isomer in the oxidized equilibrium oxidizes the minor isomer in the reduced equilibrium. If this electron transfer reaction occurs, it can interfere with the calculations of the kinetic results. However, the fact that the rate constants were observed to be independent of the concentration of the electroactive species indicates that the cross-reaction does not interfere with the analysis to any significant extent.

Table 1. Rate Constants and Thermodynamics for Linkage Isomerization of $[Ru(NH_3)_5(sulfoxide)]^{2+/3+}$ and *cis*-$[Ru(NH_3)_4L(sulfoxide)]^{2+/3+}$ in Acetone (20 °C)

$Ru^{III}S \rightarrow O$

ligand	k_1/s^{-1}	$\Delta H^{\ddagger}_1$/kJ mol^{-1}	$\Delta S^{\ddagger}_1$/J K^{-1} mol^{-1}	$\Delta G^{\ddagger}_1$/kJ mol^{-1}
dmso	0.37 ± 0.01	78.9 ± 1.0	16 ± 4	74.2
tmso	1.57 ± 0.02	81.0 ± 0.5	35 ± 2	70.7
Cl-mso	1.93 ± 0.01	77.1 ± 0.6	24 ± 2	70.1
n-buso	4.3 ± 0.2	77.4 ± 0.5	32 ± 2	68.0
benzylso	16.0 ± 0.9	72.6 ± 0.9	26 ± 3	65.0
dpso	37.8 ± 1.7	72.1 ± 1.0	31 ± 4	63.0
Cl-pso	43.8 ± 1.8	73.7 ± 0.7	38 ± 2	62.6
sos	62.9 ± 0.7	68.3 ± 0.3	23 ± 1	61.6
s-buso	(5000)	63.3 ± 1.4	42 ± 5	51.0
$(dmso)_2$	1150[a]			
(py)(dmso)	3.0 ± 0.1	76.5 ± 0.5	25 ± 2	69.2

$Ru^{II}O \rightarrow S$

ligand	k_2/s^{-1}	$\Delta H^{\ddagger}_2$/kJ mol^{-1}	$\Delta S^{\ddagger}_2$/J K^{-1} mol^{-1}	$\Delta G^{\ddagger}_2$/kJ mol^{-1}
dmso	14.3 ± 1.4	55.2 ± 0.7	−35 ± 3	65.5
tmso	10.8 ± 0.2	56.6 ± 1.0	−32 ± 4	66.0
n-buso	9.6 ± 0.6	53.1 ± 0.7	−44 ± 3	66.0
benzylso	15.9 ± 1.1	52.5 ± 1.0	−42 ± 4	64.8
sos	12.6 ± 0.7	51.5 ± 0.7	−48 ± 3	65.6
s-buso	(6.5 ± 0.7)	−		
(dmso)2	16.0 ± 1.9	58.7 ± 1.0	−22 ± 4	65.1
(py)(dmso)	0.71 ± 0.04	61.7 ± 0.9	−38 ± 3	72.8

[a] At −13 °C.

Isomerization Rates for Various Complexes. The rate constants, k_1 and k_2, were measured at −13, −5, 3, 10, 20, 30 and °C for both the $Ru^{III}S \rightarrow O$ and for the $Ru^{II}O \rightarrow S$ isomerizations of the complexes. A series of $[Ru(NH_3)_5(sulfoxide)](PF_6)_2$ (the sulfoxides are listed in Table I) and *cis*-$[Ru(NH_3)_4(L)(dmso)](PF_6)_2$ (L = py and dmso) were examined for the measurements of the $Ru^{III}S \rightarrow O$ reactions. For the measurements of the rates of $Ru^{II}O \rightarrow S$ isomerization, the corresponding compounds were electro-oxidized and used. But, we could not obtain accurate values for the complexes of Cl-mso, Cl-dpso, and *s*-buso because they were partially decomposed during the bulk electrolysis. The upper limit of the rates accessible by DPSCA is 10^3 s^{-1} [2c]. However we estimated a value of 5000 s^{-1} by extrapolation of the linear of $1/T$ vs $\ln(k/T)$ plot in the case of $Ru^{III}S \rightarrow O$ for the *s*-buso complex. Table 1 summarizes the values of the linkage isomerization rate constants at 20 °C.

The rate constants, k_1, are 0.37 s^{-1} (dmso) < 1.57 (tmso) < 4.3 (*n*-buso) < 16 (benzylso) < 38 (dpso) < 63 (sos) < 5000-(*s*-buso) for S→O isomerization in the series of $[Ru(NH_3)_5(sulfoxide)]^{3+}$. Substitution of the bulky *sec*-butyl group for the methyl group on the sulfur atom increases the rate 4 orders of magnitude for the $Ru^{III}S \rightarrow O$ change. Substitution of chlorine for hydrogen on the methyl group and on the phenyl group increases the rate, 0.37 s^{-1} (dmso) < 1.9 (Cl-mso) and 38 (dpso) < 44 (Cl-pso). The rate for the $Ru^{III}S \rightarrow O$ change increases

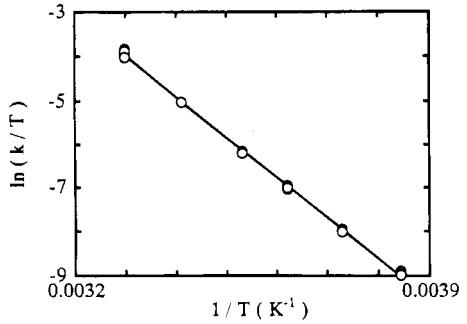

Figure 4. Temperature dependence of the rate constants for the $Ru^{III}S \rightarrow O$ isomerization of $[Ru(NH_3)_5(Cl\text{-}mso)]^{2+/3+}$ in acetone.

from 0.37 to 3.0 s^{-1} by substituting pyridine for NH_3 in the dmso complex.

The specific rates for O→S isomerization in the $[Ru(NH_3)_5(sulfoxide)]^{2+}$ series remain near 10 s^{-1}, revealing no significant difference between the complexes. However, substitution of pyridine for NH_3 in the dmso complex decreases the rate from 14 to 0.71 s^{-1}.

In *cis*-$[Ru(NH_3)_4(dmso)_2]^{2+/3+}$, rate constants were determined for EC systems of $Ru^{3+}SS \rightarrow SO$ and $Ru^{2+}OO \rightarrow SO$ and the values obtained are also entered in Table 1. The isomerization rate for $Ru^{3+}SS \rightarrow SO$ is over 1000 s^{-1} at −13 °C and is the fastest among the sulfoxide complexes measured, while the rate for $Ru^{2+}OO \rightarrow SO$ is 16 s^{-1}, similar to those for the isomerization of the pentaammine sulfoxide complexes.

Activation Parameters for Isomerizations of Various Complexes. A typical example of temperature dependence of the rate for the $[Ru(NH_3)_5(Cl\text{-}mso)]^{2+}$ is shown in Figure 4, which gives good linearity in a plot of $1/T$ vs $\ln(k_1/T)$. We obtained values of activation parameters, $\Delta H^{\ddagger}$ and $\Delta S^{\ddagger}$, on the basis of the following equation: $hk/kT = \exp(-\Delta H^{\ddagger}/RT + \Delta S^{\ddagger}/R)$. The results are tabulated in Table 1 for $\Delta H^{\ddagger}$ and $\Delta S^{\ddagger}$ with k and $\Delta G^{\ddagger}$ at 20 °C.

The values of $\Delta H^{\ddagger}$ range from 81 (tmso) to 63 kJ mol^{-1} (*s*-buso) for $Ru^{III}S \rightarrow O$ and from 62 ((py)dmso) to 52 kJ mol^{-1} (sos) for $Ru^{II}O \rightarrow S$. The $\Delta S^{\ddagger}$ values range from 16 (dmso) to 42 J K^{-1} mol^{-1} (*s*-buso) for $Ru^{III}S \rightarrow O$ and from −22 ($(dmso)_2$) to −48 JK^{-1} mol^{-1} (sos) for $Ru^{II}O \rightarrow S$. The activation entropies are positive for $Ru^{III}S \rightarrow O$ and negative for $Ru^{II}O \rightarrow S$.

A striking result is the reversal of the sign of $\Delta S^{\ddagger}$ for the isomerization on Os(III) and Os(II),[15a] which suggests that an important factor in determining $\Delta S^{\ddagger}$ is the difference in polarity at the two points of attachment. The O site being more negative will interact more strongly with the solvent, and solvent disorder will increase when S rather than O is exposed to the solvent. This effect will be reflected, at least in part in the transition state for $Ru^{III}S \rightarrow O$, hence the positive value of $\Delta S^{\ddagger}$. In the process $Ru^{II}O \rightarrow S$, the reverse is true.

Homogeneous Oxidation for $[Ru(NH_3)_5(sulfoxide)]^{2+}$. In spite of what the electrochemical results might suggest, we found that any (sulfoxide)ruthenium(II) complexes are capable of acting as reasonably good homogeneous reducing agents. When an acetone solution of the sos complex is added to 1 equiv of $[Ru(NH_3)_5(PhF2\text{-}CN)]^{3+}$ (PhF2-CN = 2,6-difluorobenzonitrile), the solution turns deep yellow, indicating the formation of $[Ru(NH_3)_5(PhF2\text{-}CN)]^{2+}$, even though the reduction potential of the 2,6-difluorobenzonitrile complex ($E_{1/2}$ = 0.68 V in acetone) is substantially negative in relation to that of the oxidation wave (0.97 V) of the sulfoxides, even at low scan rates. This qualitative observation was confirmed by electrochemical experiments that showed the reduction of the $[Ru(NH_3)_5(PhF2\text{-}CN)]^{3+}$ to be virtually complete within one hour as shown in eq 1.

$$[Ru(NH_3)_5(S)]^{2+} + [Ru(NH_3)_5(PhF2\text{-}CN)]^{3+} \rightarrow [Ru(NH_3)_5(O)]^{3+} + [Ru(NH_3)_5(PhF2\text{-}CN)]^{2+} \quad (1)$$

Harman and Taube[15a,b] found the same redox reaction in osmium(II) ammine complexes and devised the following method to calculate equilibrium constants for isomerizations. When the above experiment is performed with the *p*-fluorobenzonitrile analogue ($E_{1/2}$ = 0.585 V) in acetone, a measurable equilibrium is gradually established in which approximately three-fifths of the Ru(II) is in the form of the (*p*-fluorobenzonitrile)pentaammine complex, $[Ru(NH_3)_5(PhF\text{-}CN)]^{2+}$. When the relative concentrations of the four ruthenium species in solution are measured, a value of 0.43 is calculated for the equilibrium constant K_{eq} where

$$K_{eq} = \frac{[Ru(NH_3)_5(PhF\text{-}CN)]^{3+}[Ru(NH_3)_5(S)]^{2+}}{[Ru(NH_3)_5(PhF\text{-}CN)]^{2+}[Ru(NH_3)_5(O)]^{3+}}$$

This leads to a value of E_{eq} = 0.564 V (NHE) in acetone for the half-reaction

$$[Ru(NH_3)_5(O)]^{3+} + e^- \rightarrow [Ru(NH_3)_5(S)]^{2+}$$

in which each member of the couple is in its stable state.

Consideration of the redox potentials for the S-bound isomer along with the above result yields the isomerization energy for ruthenium(III) in acetone as follows:

$$[Ru(NH_3)_5(S)]^{3+} + e^- = [Ru(NH_3)_5(S)]^{2+} \ (0.94 \text{ V}) \ (-F)$$
$$(-)\ [Ru(NH_3)_5(O)]^{3+} + e^- = [Ru(NH_3)_5(S)]^{2+} \ (0.56 \text{ V}) \ (-F)$$
$$[Ru(NH_3)_5(S)]^{3+} = [Ru(NH_3)_5(O)]^{3+} \ (0.38 \text{ V}) \ (-F)$$

A standard free energy of −37 kJ mol^{-1} at 20 °C corresponds to an equilibrium constant of 3×10^6 for

$$[Ru(NH_3)_5(S)]^{3+} \rightleftarrows [Ru(NH_3)_5(O)]^{3+}$$

This value together with that of k_1 leads to a specific rate of $k_{-1} = 2 \times 10^{-5}$ s^{-1} for $Ru^{3+}O \rightarrow S$ isomerization. The same treatment has been applied to

$$[Ru(NH_3)_5(O)]^{2+} \rightleftarrows [Ru(NH_3)_5(S)]^{2+}$$

which gives $\Delta G1 = -54$ kJ mol^{-1}, $K_1 = 4 \times 10^9$, and $k_{-1} = 3 \times 10^{-9}$. The same experiments were performed for the dmso and the *n*-buso complexes. These results are summarized in Table 2.

Energy Relationship of ECEC for $[Ru(NH_3)_5sulfoxide]^{2+/3+}$. In the isomerization of Ru(III), the values of $\Delta G1$ and $\Delta G^{\ddagger}1$ are different for the dmso, the *n*-buso, and the sos complexes. However, we find that the kinetic free energy barrier to S→O isomerization on Ru^{III} (this is given by $(\Delta G_1 - \Delta G^{\ddagger}_1)$) is almost identical for the three complexes. While O→S isomerization on Ru(III), involving as it does stable species changing to unstable, is not directly measurable, the same change for Ru(II) takes an unstable form to a stable one. We find that the rates of the O→S changes on both centers are almost independent of the steric bulk of the substituents on the S in both cases.

(15) (a) Harman, W. D.; Taube, H. *J. Am. Chem. Soc.* **1988**, *110*, 5403. (b) Harman, W.D.; Sekine, M.; Taube, H. *J. Am. Chem. Soc.* **1988**, *110*, 2439.

Table 2. Thermodynamic Parameters of $[Ru(NH_3)_5(sulfoxide)]^{2+/3+}$ Linkage Isomerizations at 20 °C

	$Ru^{III}S \rightarrow O$				
ligand	K_1	k_1/s^{-1}	k_{-1}/s^{-1}	ΔG_1/kJ mol^{-1}	$\Delta G^{\ddagger}_1$/kJ mol^{-1}
dmso	2×10^4	0.37	2×10^{-5}	−24	74
n-buso	4×10^5	4.3	1×10^{-5}	−32	68
sos	3×10^6	63	2×10^{-5}	−37	62
	$Ru^{II}O \rightarrow S$				
ligand	K_2	k_2/s^{-1}	k_{-2}/s^{-1}	ΔG_2/kJ mol^{-1}	$\Delta G^{\ddagger}_2$/kJ mol^{-1}
dmso	2×10^{11}	14	1×10^{-10}	−63	66
n-buso	4×10^9	9.6	2×10^{-9}	−54	66
sos	4×10^9	13	3×10^{-9}	−54	66

The relief of strain in the activated complex is measured to be the same as that measured for the overall change. A similar pattern has been observed[15a] in studying the dynamics of linkage isomerization for $Os(NH_3)_5^{3+/2+}$ in changing between a position on the aromatic ring to the polar groups of NH_2 or $N(CH_3)_2$ as substituents on the ring. But in these cases participation in the activated complex by the polar group when $Os(NH_3)_5^{3+}$ is transferrring to it from a 2:3 position on the ring is unlikely. In the system we have studied, the two sites are adjacent, and even in this case, in the O→S isomerization, the steric effects of the substituents on the ring are not sensed in the activated complex. The energetics for the three cases are shown schematically in Figure 5.

Electrochemical Scheme of *cis*-$[Ru(NH_3)_4(dmso)_2]^{2+/3+}$. We now consider the electrochemical scheme for *cis*-$[Ru(NH_3)_4(dmso)_2]^{2+/3+}$. In order to determine thermodynamics in the scheme, we need some values for redox potentials, rates, and equilibrium constants.

We obtained the redox potentials for

$$[Ru(NH_3)_4(O)(S)]^{2+} \rightarrow [Ru(NH_3)_4(O)(S)]^{3+} + e^- \qquad E_{1/2} = 0.82 \text{ V}$$

and

$$[Ru(NH_3)_4(O)(O)]^{2+} \rightarrow [Ru(NH_3)_4(O)(O)]^{3+} + e^- \qquad E_{1/2} = 0.04 \text{ V}$$

We also determined the value of E_{pa} 0.82 V (100 mV s^{-1}) for

$$[Ru(NH_3)_4(S)(S)]^{2+} \rightarrow [Ru(NH_3)_4(S)(S)]^{3+} + e^-$$

The rates of linkage isomerizations for $Ru^{II}OO \rightarrow OS$ and $Ru^{III}SS \rightarrow SO$ are 16 s^{-1} and over 1000 s^{-1} at 20 °C by the DPSCA experiments. In order to determine rates for $Ru^{II}OS \rightarrow SS$ and $Ru^{III}SO \rightarrow SS$ isomerizations, we carried out a digital simulation. In the simulation, we need equilibrium constants for

$$[Ru(NH_3)_4(S)(S)]^{3+} \rightleftarrows [Ru(NH_3)_4(S)(O)]^{3+}$$

and

$$[Ru(NH_3)_4(O)(O)]^{2+} \rightleftarrows [Ru(NH_3)_4(O)(S)]^{2+}$$

We roughly estimated both equilibrium constants over 100 on the basis of rotating electrode voltammograms of the *cis*-$[Ru(NH_3)_4(dmso)_2]^{2+}$ and *cis*-$[Ru(NH_3)_4(dmso)_2]^{3+}$. Then the digital simulation was carried out for the isomerizations $Ru^{II}OS \rightarrow SS$ and $Ru^{III}SO \rightarrow OO$. The result of the best fit is shown in Figure 2C which is to be compared to the experimental trace in Figure 2A. We roughly estimate the rates 0.04 and 0.01 s^{-1} for $Ru^{II}OS \rightarrow SS$ and for $Ru^{III}SO \rightarrow OO$, respectively, which are significantly slower than those for the $Ru^{II}OO \rightarrow OS$ and $Ru^{III}SS \rightarrow SO$, respectively.

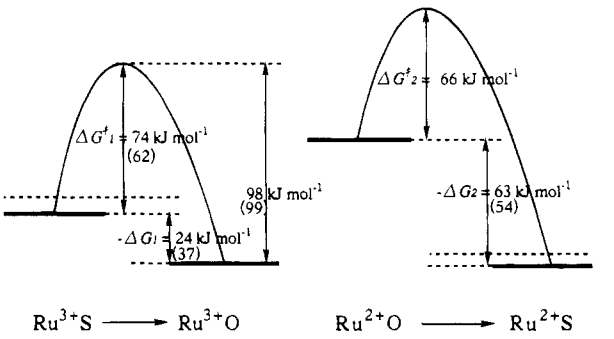

Figure 5. Energy relationships of the isomerizations for $[Ru(NH_3)_5(dmso)]^{2+/3+}$ in acetone at 20 °C. The values in parentheses are for $[Ru(NH_3)_5(sos)]^{2+/3+}$.

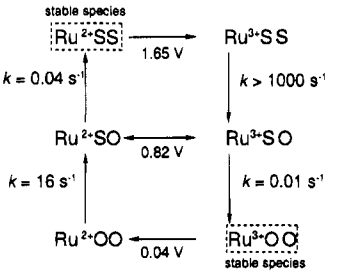

Figure 6. Rate parameters for the "double square" reaction scheme for *cis*-$[Ru(NH_3)_4(dmso)_2]^{2+/3+}$ at 20 °C.

We summarize the electrochemical scheme of *cis*-$[Ru(NH_3)_4(dmso)_2]^{2+/3+}$ in Figure 6.

Summary

We characterized the redox behaviors for the $[Ru(NH_3)_5(sulfoxide)]^{2+/3+}$ and *cis*-$[Ru(NH_3)_4(dmso)_2]^{2+/3+}$ and then obtained the first-order rate constants of the linkage isomerizations. In the isomerization of $Ru^{III}S \rightarrow O$, a bulky substituent group at the S atom accelerates the reaction over 1000 s^{-1} in $[Ru(NH_3)_5(sulfoxide)]^{3+}$. The rate of the dmso complex, 0.3 s^{-1}, is the slowest. In the *cis*-$[Ru(NH_3)_4(dmso)_2]^{3+}$, the rate of the $Ru^{III}SS \rightarrow SO$ is much faster than 1000 s^{-1} at room temperature.

Substitution of the S atom hardly changes the reaction rates for the $Ru^{II}O \rightarrow S$ of the $[Ru(NH_3)_5(sulfoxide)]^{2+}$ complexes (~10 s^{-1}). However, the rate of the *cis*-$[Ru(NH_3)_4(py)(dmso)]^{2+}$ gives 0.7 s^{-1}.

We obtained the thermodynamic parameters in the dmso, the *n*-buso, and the sos complexes and also determined the reaction scheme. The isomerization rates in the *cis*-$[Ru(NH_3)_4(dmso)_2]^{2+/3+}$ are determined to be 0.04 and 0.01 s^{-1} for $Ru^{II}OS \rightarrow SS$ and for $Ru^{III}SO \rightarrow OO$, respectively, with digital simulations.

Acknowledgment. We are grateful to Professor Henry Taube for his encouragement and insight. We also acknowledge Dr. Akio Ichimura of Osaka City University for measuring the thin layer cyclic voltammograms. Partial support of this work by the Yazaki Foundation and the Nihon Shoken Foundation is gratefully acknowledged.